Electronic Supplementary Information (ESI)

Efficient Detection of Fe(III) and Chromate Ions in Water by Two Robust Lanthanide Metal-Organic Frameworks

Jian-Peng Dong, Bo Li,* Yu-Jie Jin and Li-Ya Wang*

College of Chemistry and Pharmaceutical Engineering, Nanyang Normal University, Nanyang 473061, People's Republic of China.

Corresponding authors:

*(B. Li) E-mail: libony0107@nynu.edu.cn

*(L. Y. Wang) E-mail: wly@nynu.edu.cn

Experimental Section

Materials and Instrumentations

All of the materials were commercially available and used without further purification. All the solvents used were of analytical grade. Powder X-ray diffraction (PXRD) data of the samples were collected on a D/MAX-3D diffractometer with Cu Kα radiation (λ=1.5418 Å) over the 2θ range of 5°–50° at the scan rate of 5° min^{-1} at room temperature. Simulation of the PXRD spectra was carried out with the single-crystal data and diffraction crystal module of the Mercury program available free of charge via http://www.ccdc.cam.ac.uk/mercury/. Thermogravimetry analyses (TGA) were performed on a TA Q50 system under a N_2 atmosphere (flow rate = 60 mL min^{-1}) in the temperature range 25-700 °C at a heating rate of 10 °C min^{-1}. Elemental analyses of C, H and N for all samples were collected on a Perkin-Elmer 240 analyzer. Fourier-transform infrared spectra (FT-IR) were recorded on a Shimadzu IR Tracer-100 by using KBr pellets (4000-400 cm^{-1}). UV-vis diffuse reflectance spectra were recorded with a Shimadzu UV-2600 UV-vis spectrophotometer. Luminescence spectra and lifetime decays were collected on an Edinburgh FLS980 fluorescence spectrophotometer. The quantum yields (QYs) of **1-Eu** and **1-Tb** were measured using a $BaSO_4$-coated integrating sphere and calculated through an absolute method.[1] All photographs were taken with a Canon EOS 80D camera.

X-Ray crystallography

Single-crystal X-ray diffraction (SCXRD) measurements were performed on a Rigaku XtaLAB Pro diffractometer with Cu-Kα radiation (λ = 1.54178 Å) at 200/293 K. The SADABS program was used for absorption correction.[2] All the structures were solved by direct methods and refined by the full-matrix least-squares method on F^2 with SHELXS and SHELXL programs.[3] The hydrogen atoms on ligands were placed in calculated positions and refined using the riding model. The hydrogens attached to water molecules were located from the difference Fourier maps and refined isotropically. Because guest solvent molecules H_2O in the frameworks were highly disordered, the diffused contributions from them were removed by the SQUEEZE routine in PLATON. The final formula of complexes were determined by means

of single-crystal structure, TGA and elemental analysis. Refinement parameters and crystallographic data are listed in Table S1-S3 (Supporting Information).

Syntheses of $\{[Ln(L)(H_2O)]\cdot 7H_2O\}_n$ (Ln = Eu, Tb)

The mixture solution of H_3L (0.05 mmol), $Eu(NO_3)_3\cdot 6H_2O$ (0.1 mmol), DMF (3 mL), H_2O (2 mL) and HNO_3 (0.1 mL) was stirred for 30 min, then transferred to a Teflon-lined stainless steel vessel then heated at 150 °C for 72 h. After cooled to room temperature at a rate of 5 °C min^{-1}, the resulting colorless crystals were harvested by filtration, washed with distilled water, and then dried in air to furnish **1-Eu**. Other complexes were synthesized similarly to **1-Eu**, except $Tb(NO_3)_3\cdot 6H_2O$ in place of Eu(III) nitrate.

$\{[Eu(L)(H_2O)]\cdot 7H_2O\}_n$ (**1-Eu**). Yield: 64.5% (based on H_3L). $C_{14}H_{22}EuNO_{14}$ (Mr = 580.17). Elemental analysis calcd: C 28.96, H 3.79, N 2.41 %. Found: C 28.98, H 3.85, N 2.48 %.

$\{[Tb(L)(H_2O)]\cdot 7H_2O\}_n$ (**1-Tb**). Yield: 62.6% (based on H_3L). $C_{14}H_{22}TbNO_{14}$ (Mr = 587.13). Elemental analysis calcd: C 28.61, H 3.75, N 2.38 %. Found. C 28.87, H 3.81, N 2.42 %.

Luminescence Sensing Experiments

In particular, 2.0 mg of powder sample was added into 3.0 mL of deionized water of $M(NO_3)_x$ (M = Ca^{2+}, Ag^+, Mg^{2+}, K^+, Na^+, Mn^{2+}, Cr^{3+}, Pb^{2+}, Cd^{2+}, Fe^{2+}, Zn^{2+}, Al^{3+}, Bi^{3+}, Co^{2+}, Ni^{2+}, Cu^{2+}, and Fe^{3+}) and KX (X = X = Cl^-, Br^-, I^-, IO_3^-, SCN^-, PO_4^{3-}, NO_3^-, CO_3^{2-}, SO_4^{2-}, $H_2PO_4^-$, MnO_4^-, OH^-, Ac^-, CrO_4^{2-}, $Cr_2O_7^{2-}$) at the same concentration (1 mM). Then, the mixtures were ultrasonicated for 10 min to form a suspension, followed by recording of the luminescent spectra under the same conditions.

Table S1. Crystal data and structural refinement parameters for **1-Eu** and **1-Tb.**

	1-Eu	**1-Tb**
CCDC number	2045548	2045549
Formula	$C_{14}H_{22}EuNO_{14}$	$C_{14}H_{22}TbNO_{14}$
Formula weight	580.17	587.13
T / K	293(2)	293(2)
Space group	$I4_1/a$	$I4_1/a$
Crystal system	Tetragonal	Tetragonal
a / Å	25.3668(2)	25.3649(10)
b / Å	25.3668(2)	25.3649(10)
c / Å	15.1922(2)	15.2716(10)
α / deg	90	90
β / deg	90	90
γ / deg	90	90
V / Å^3	9775.8(2)	9825.41(10)
Z	16	16
D_{calc} (g cm^{-3})	1.234	1.247
Reflections collected	12876	13665
Independent reflections	4805	4819
R(int)	0.0340	0.0272
F(000)	3488	3520

GOF on F^2	1.086	1.105
R_1[a], wR_2[b] [$I > 2\sigma(I)$]	0.0473, 0.1809	0.0607, 0.2499
R_1[a], wR_2[b] (all data)	0.0503, 0.1843	0.0642, 0.2579
[a]$R_1 = \Sigma\|\|F_o\| - \|F_c\|\|/\Sigma\|F_o\|$. [b]$wR_2 = [\Sigma w(F_o^2 - F_c^2)^2/\Sigma w(F_o^2)^2]^{1/2}$.		

Table S2. Selected bond lengths (Å) and angles (°) for **1-Eu**.

Eu1-O1	2.426(4)	Eu1-O3#2	2.355(3)	Eu1-O4#1	2.308(4)
Eu1-O2	2.488(4)	Eu1-O6#3	2.464(3)	Eu1-O7	2.433(4)
Eu1-O6#4	2.617(3)	Eu1-N1#3	2.581(4)	Eu1-O5#4	2.575(4)
O3#2-Eu1-O1	82.76(13)	O4#1-Eu1-O1	94.08(14)	O4#1-Eu1-O3#2	144.24(14)
O1-Eu1-O7	132.96(13)	O3#2-Eu1-O7	79.13(14)	O4#1-Eu1-O7	77.28(14)
O1-Eu1-O6#3	75.48(12)	O3#2-Eu1-O6#3	138.81(12)	O4#1-Eu1-O6#3	72.82(13)
O3#2-Eu1-O2	76.85(13)	O4#1-Eu1-O2	73.03(15)	O7-Eu1-O6#3	140.19(14)
O6#3-Eu1-O2	114.20(12)	O7-Eu1-O2	80.43(13)	O1-Eu1-O2	53.17(12)
O1-Eu1-O5#4	142.47(13)	O3#2-Eu1-O5#4	125.17(12)	O4#1-Eu1-O5#4	76.96(15)
O2-Eu1-O5#4	147.53(15)	O6#3-Eu1-O5#4	67.03(13)	O7-Eu1-O5#4	81.17(15)
O1-Eu1-N1#3	78.58(13)	O3#2-Eu1-N1#3	78.53(13)	O4#1-Eu1-N1#3	135.95(13)
O2-Eu1-N1#3	127.74(13)	O6#3-Eu1-N1#3	63.25(12)	O7-Eu1-N1#3	137.72(13)
O3#2-Eu1-O6#4	75.46(11)	O4#1-Eu1-O6#4	120.32(13)	O5#4-Eu1-N1#3	83.07(15)
O6#3-Eu1-O6#4	102.75(10)	O7-Eu1-O6#4	70.73(12)	O1-Eu1-O6#4	143.86(12)
N1#3-Eu1-O6#4	69.14(12)	O5#4-Eu1-O6#4	49.74(12)	O2-Eu1-O6#4	143.05(12)
Symmetry transformations used to generate equivalent atoms: #1 *y*-1/4, -*x*+5/4, -*z*+1/4; #2 -*x*+1, -*y*+1, -z; #3 *y*-1/4, -*x*+3/4, *z*-1/4; #4 -*x*+1/2, -*y*+1, *z*-1/2.					

Table S3. Selected bond lengths (Å) and angles (°) for **1-Tb**.

Tb1-O1	2.396(4)	Tb1-O5#2	2.326(4)	Tb1-O6#1	2.295(4)
Tb1-O2	2.505(4)	Tb1-O3#3	2.443(4)	Tb1-O7	2.391(5)
Tb1-O3#4	2.625(4)	Tb1-N1#3	2.575(5)	Tb1-O4#4	2.523(5)
O6#1-Tb1-O1	94.39(17)	O6#1-Tb1-O7	78.16(17)	O6#1-Tb1-O3#3	72.42(15)
O6#1-Tb1-O5#2	144.96(16)	O5#2-Tb1-O7	79.56(17)	O5#2-Tb1-O3#3	138.27(15)
O5#2-Tb1-O1	82.23(15)	O1-Tb1-O7	134.20(16)	O1-Tb1-O3#3	75.26(14)
O7-Tb1-O3#3	140.08(17)	O7-Tb1-O2	82.14(16)	O1-Tb1-O4#4	142.82(16)
O6#1-Tb1-O2	72.90(16)	O3#3-Tb1-O2	113.21(14)	O7-Tb1-O4#4	80.24(18)
O5#2-Tb1-O2	77.55(15)	O6#1-Tb1-O4#4	77.62(17)	O3#3-Tb1-O4#4	67.68(15)
O1-Tb1-O2	52.92(15)	O5#2-Tb1-O4#4	124.42(15)	O2-Tb1-O4#4	148.14(17)
O6#1-Tb1-N1#3	135.96(16)	O3#3-Tb1-N1#3	63.74(15)	O5#2-Tb1-O3#4	73.89(14)
O5#2-Tb1-N1#3	77.83(16)	O2-Tb1-N1#3	127.98(16)	O1-Tb1-O3#4	142.52(15)
O1-Tb1-N1#3	78.84(15)	O4#4-Tb1-N1#3	82.23(18)	O7-Tb1-O3#4	69.40(14)
O7-Tb1-N1#3	136.02(16)	O6#1-Tb1-O3#4	121.64(15)	O3#3-Tb1-O3#4	104.20(12)
O2-Tb1-O3#4	142.58(14)	O4#4-Tb1-O3#4	50.54(14)	N1#3-Tb1-O3#4	68.28(15)
Symmetry transformations used to generate equivalent atoms: #1 *y*-1/4, -*x*+1/4, -*z*+1/4; #2 -*x*, -*y*+1, -*z*; #3 *y*-1/4, -*x*+3/4, *z*-1/4; #4 -*x*+1/2, -*y*+1, *z*-1/2.					

Table S4. Results of Continuous Shape Measure Analysis by applying SHAPE 2.1[4] for EuNO8 unit in **1-Eu**.[a]

Geometry	**1-Eu**
EP-9	33.726
OPY-9	21.949
HBPY-9	17.723
JTC-9	15.308
JCCU-9	10.866
CCU-9	10.122
JCSAPR-9	2.534
CSAPR-9	1.747
JTCTPR-9	3.166
TCTPR-9	2.550
JTDIC-9	13.864
HH-9	10.688
MFF-9	1.356

[a]The values are Continuous Shape Measure (CShM) parameters and CShM=0 for the ideal geometry and increases with the increase of the degree of distortion. EP-9 corresponds to Enneagon. OPY-9 corresponds to Octagonal pyramid. HBPY-9 corresponds to Heptagonal bipyramid. JTC-9 corresponds to Johnson triangular cupola J3. JCCU-9 corresponds to Capped cube J8. CCU-9 corresponds to Spherical-relaxed capped cube. JCSAPR-9 corresponds to Capped square antiprism J10. CSAPR-9 corresponds to Spherical capped square antiprism. JTCTPR-9 corresponds to Tricapped trigonal prism J51. TCTPR-9 corresponds to Spherical Tricapped trigonal prism. JTDIC-9 corresponds to Tridiminished icosahedron J63. HH-9 corresponds to Hula-hoop. MFF-9 corresponds to Muffin.

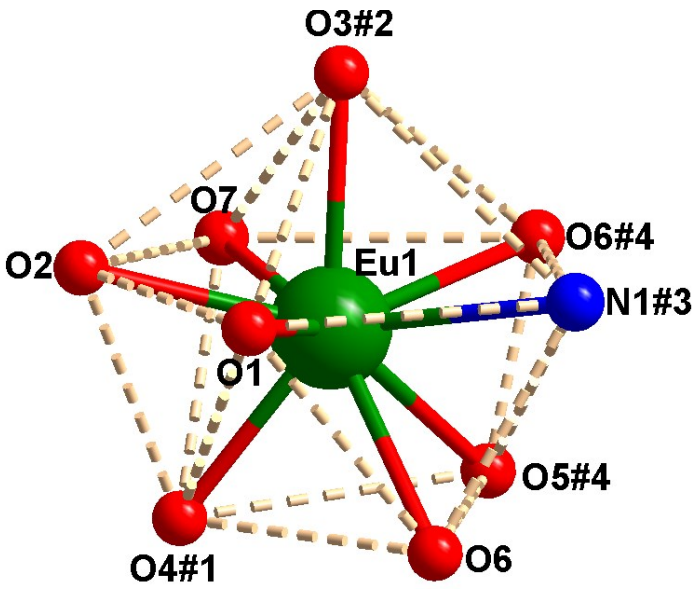

Fig. S1 Coordination geometry of the Eu^{3+} ion in **1-Eu**. Symmetry codes: #1 *y*-1/4, -*x*+5/4, -*z*+1/4; #2 -*x*+1, -*y*+1, -*z*; #3 *y*-1/4, -*x*+3/4, *z*-1/4; #4 -*x*+1/2, -*y*+1, *z*-1/2.

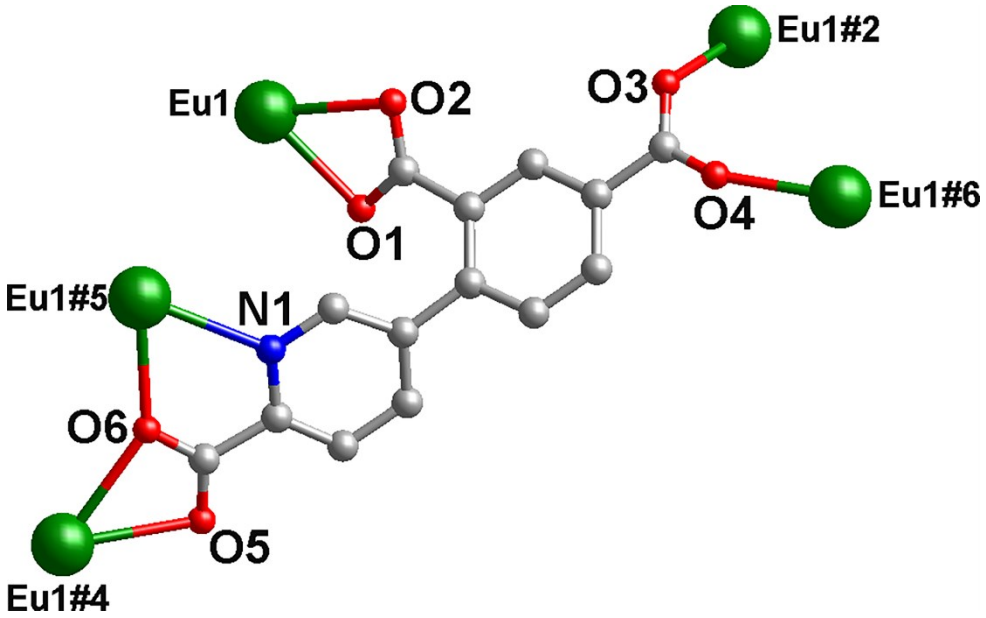

Fig. S2 Coordination mode of the ligand in **1-Eu**. Symmetry codes: #2 -*x*+1, -*y*+1, -*z*; #4 -*x*+1/2, -*y*+1, *z*-1/2; #5 -*y*+3/4, *x*+1/4, *z*+1/4; #6 -*y*+5/4, *x*+1/4, -*z*+1/4.

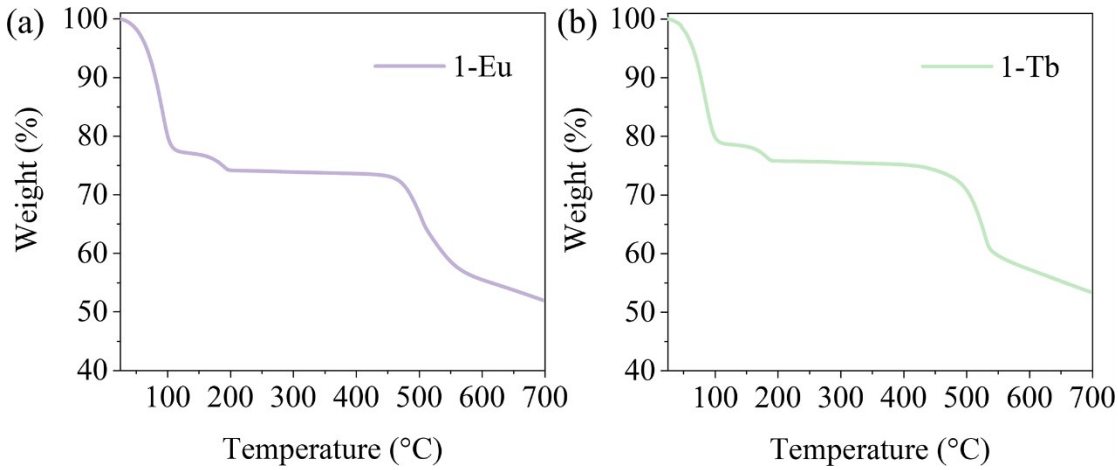

Fig. S3 Thermogravimetric analysis of **1-Eu** (a) and **1-Tb** (b).

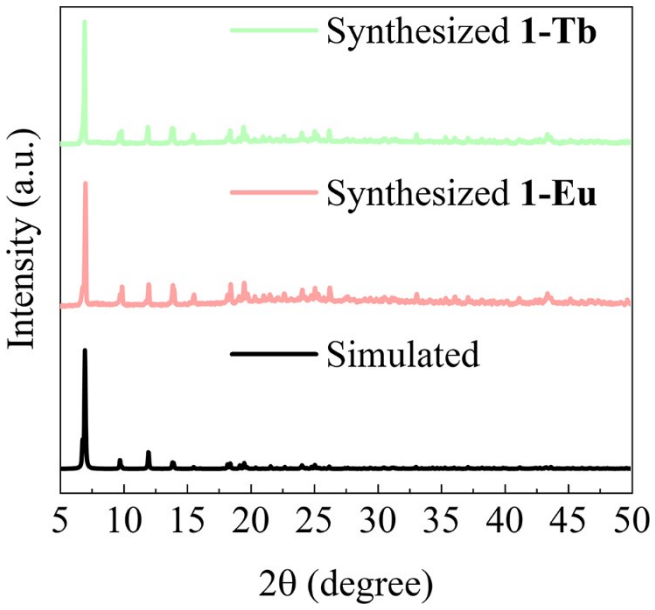

Fig. S4 PXRD patterns of **1-Eu** and **1-Tb**.

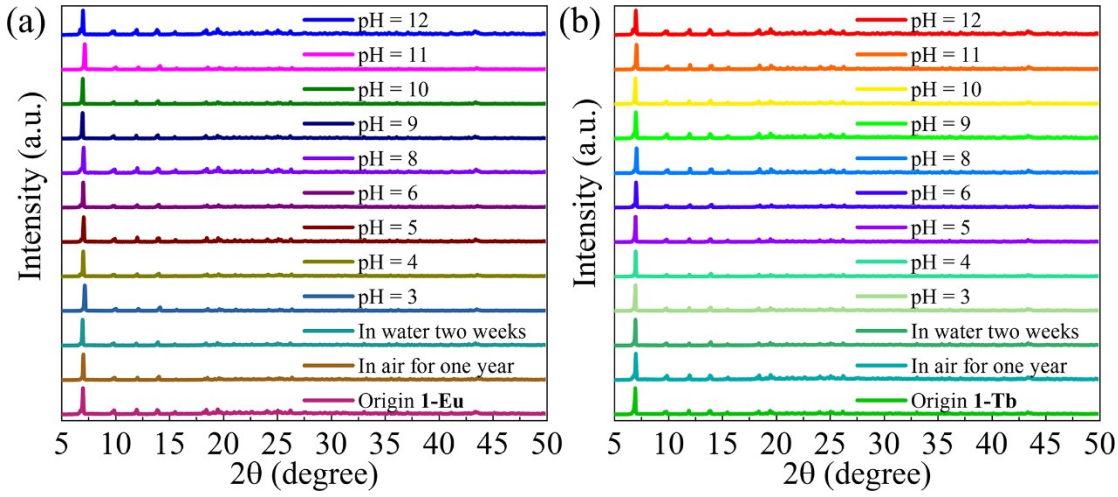

Fig. S5 PXRD patterns of **1-Eu** and **1-Tb** after treatment with different conditions.

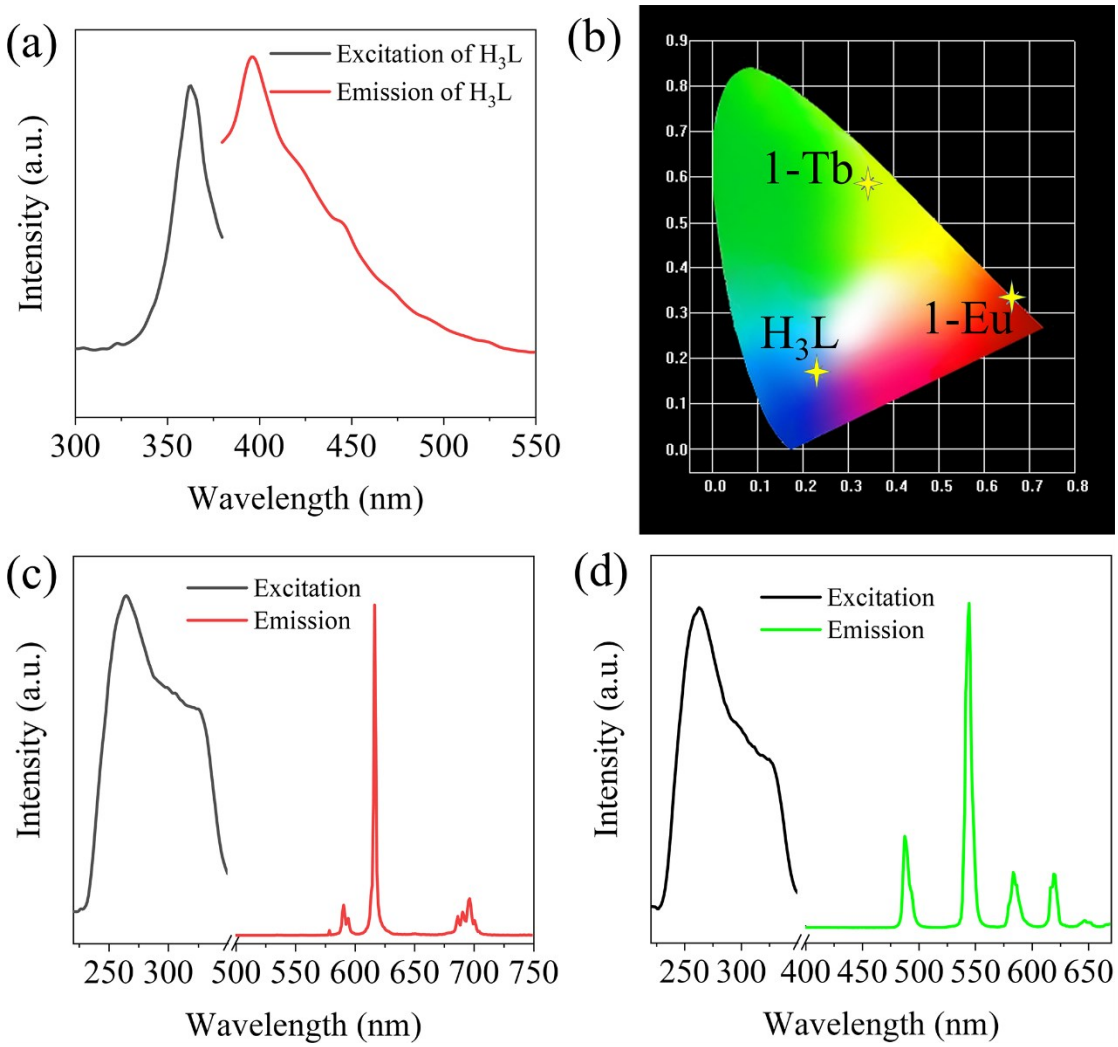

Fig. S6 (a) Excitation and emission spectra of H_3L. (b) CIE chromaticity diagram of H_3L, **1-Eu** and **1-Tb**. (c) Excitation and emission spectra of **1-Eu** and **1-Tb** (d).

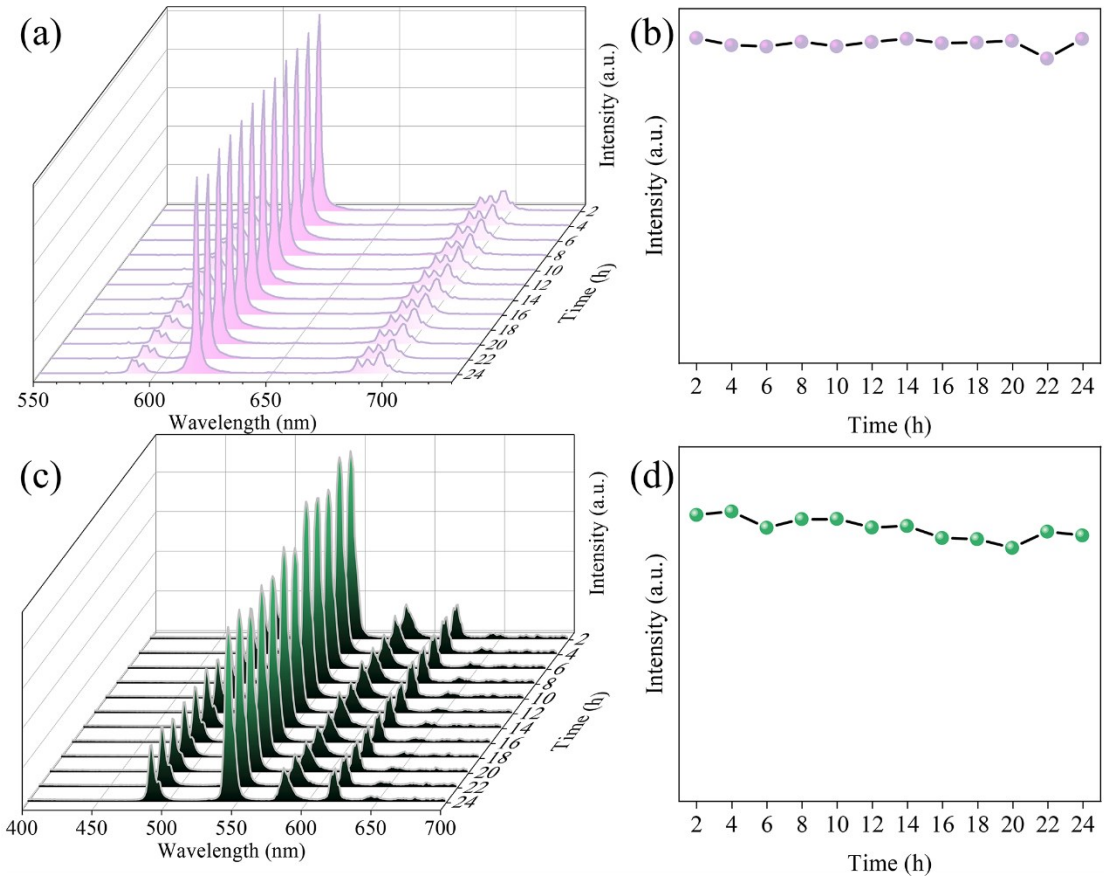

Fig. S7 (a, b) The emission spectra and emission intensities at 617 nm of **1-Eu** after immersion in water for different times. (c, d) The emission spectra and emission intensities at 545 nm of **1-Tb** after immersion in water for different times.

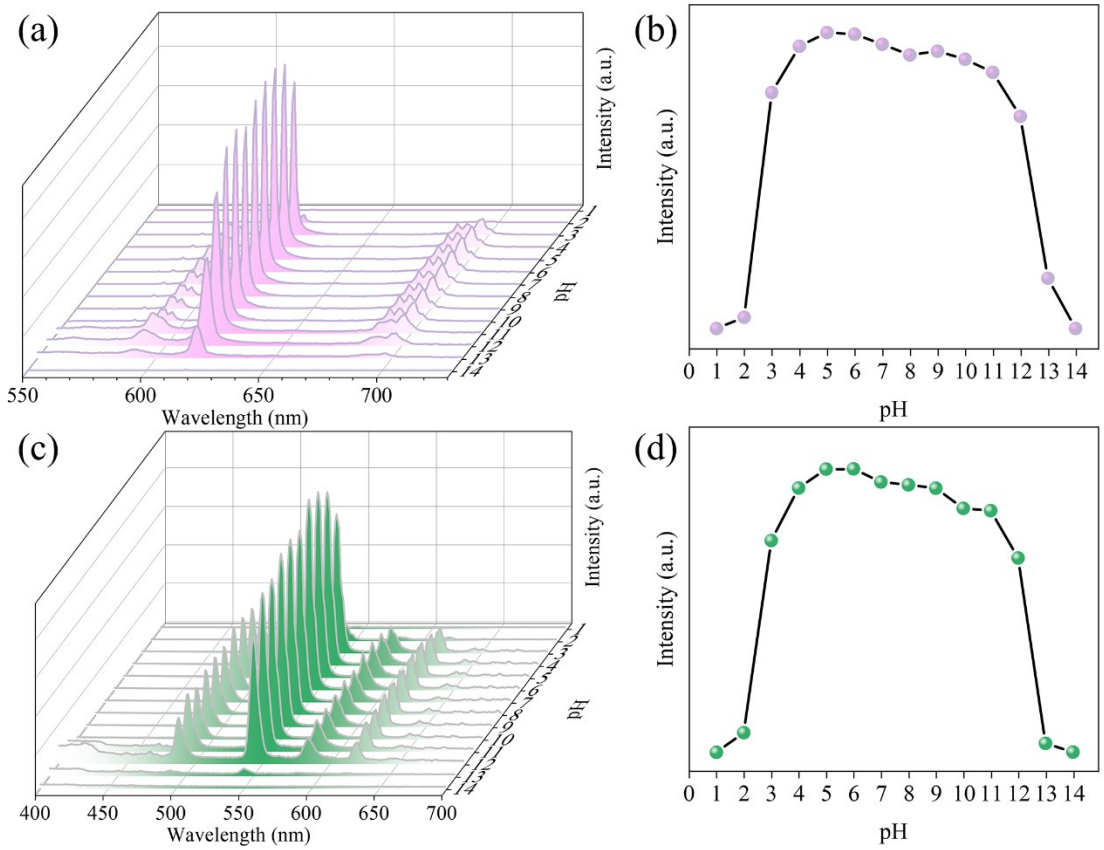

Fig. S8 (a, b) The emission spectra and emission intensities at 617 nm of **1-Eu** in aqueous solutions with different pH values (1-14). (c, d) The emission spectra and emission intensities at 545 nm of **1-Tb** in aqueous solutions with different pH values (1-14).

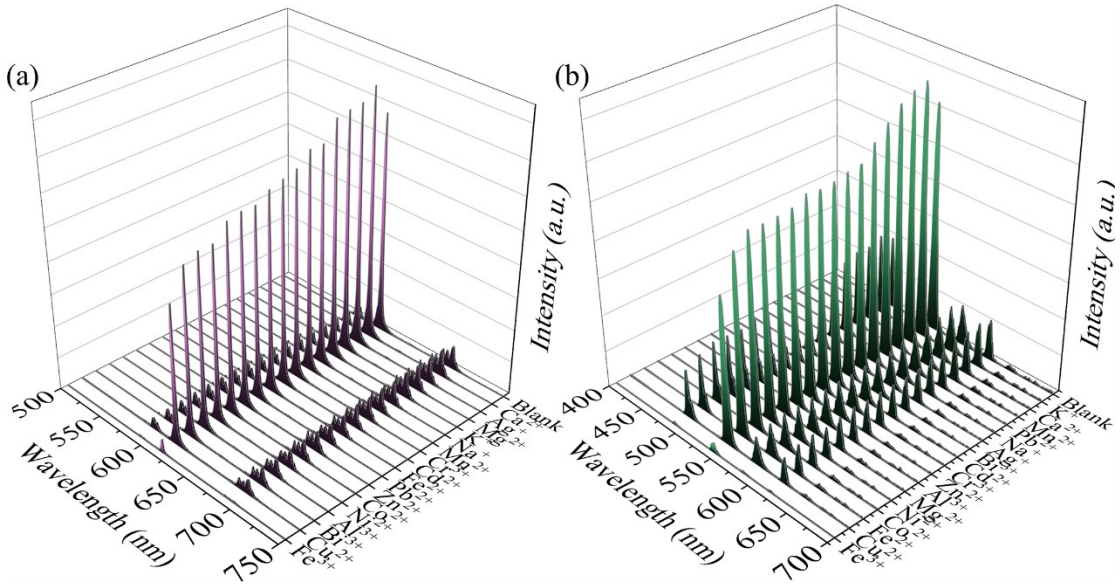

Fig. S9 Emission spectra of **1-Eu** (a) and **1-Tb** (b) immersed in cation aqueous solutions.

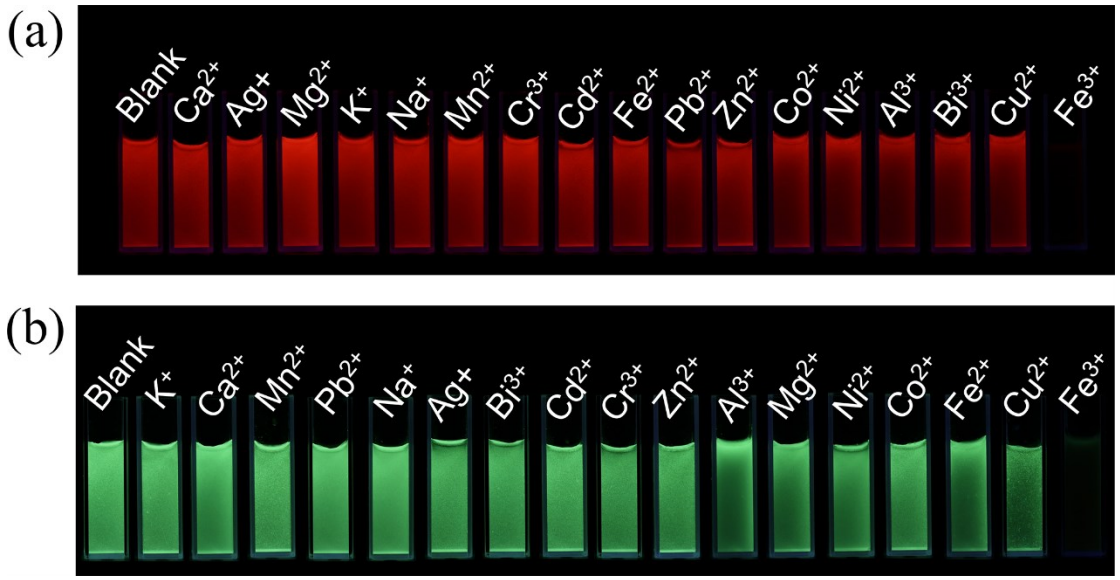

Fig. S10 The photographs of the aqueous dispersed **1-Eu** (a) and **1-Tb** (b) in the presence of different cations under UV irradiation.

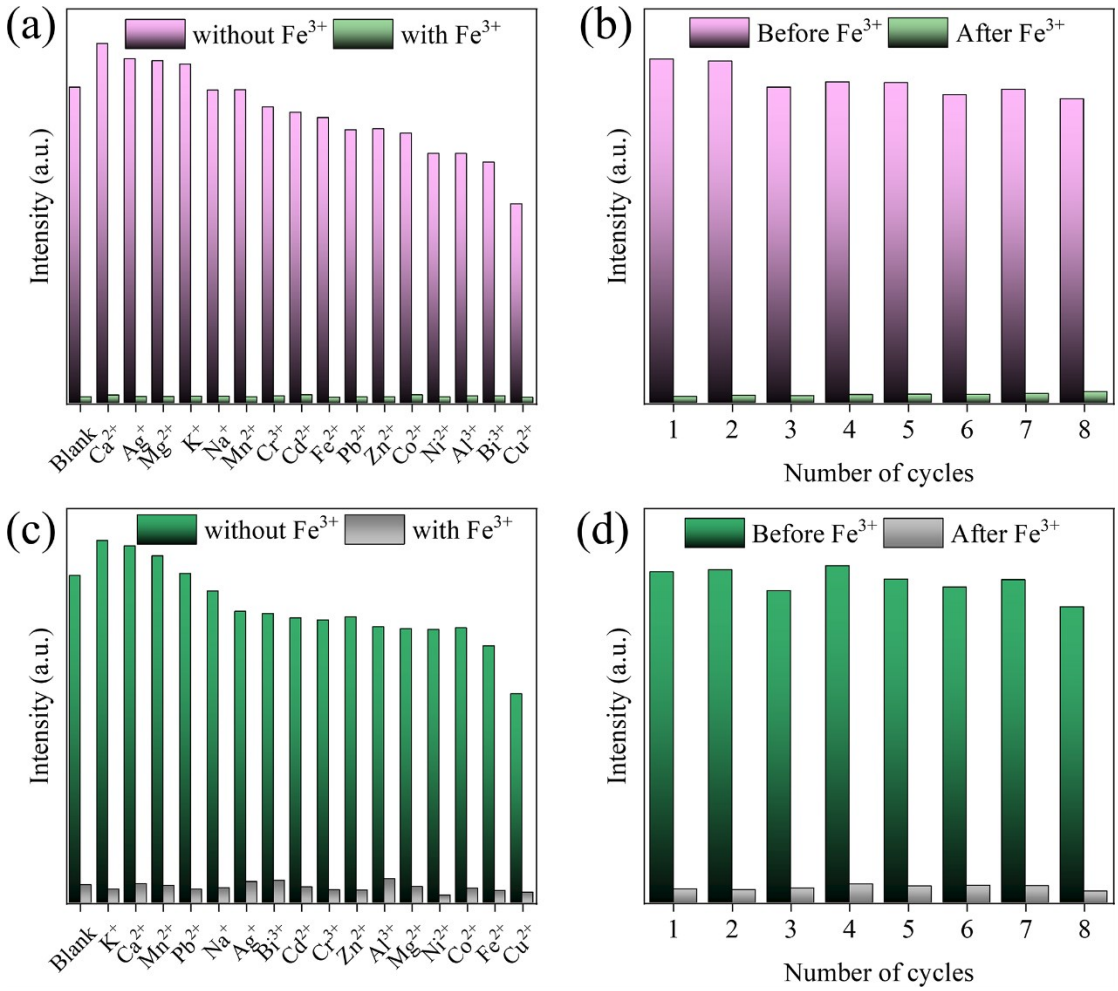

Fig. S11 (a) Luminescent responses of **1-Eu** with mixed-cations (1 mM) in aqueous solutions. (b) Eight cycles test by measuring the luminescent intensity at 617 nm of **1-Eu** before and after the adding of Fe^{3+} (1 mM). (c) Luminescent responses of **1-Tb** with mixed-cations (1 mM) in aqueous solutions. (d) Eight cycles test by measuring the luminescent intensity at 545 nm of **1-Tb** before and after the adding of Fe^{3+} (1 mM).

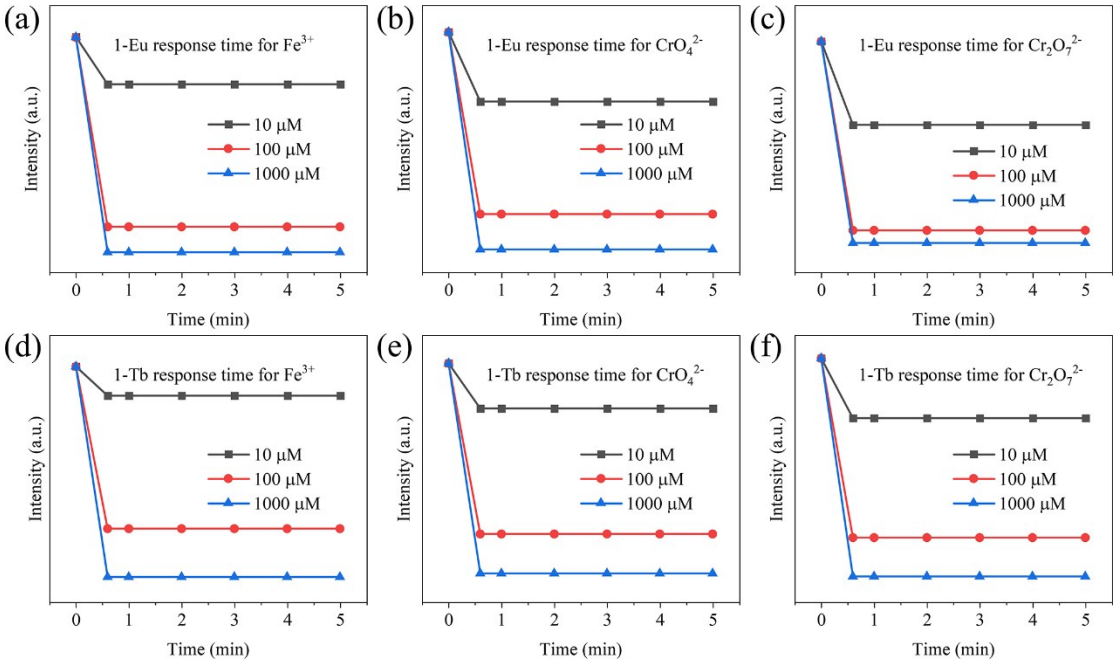

Fig. S12 Effects of response time on the fluorescent intensities at 617 nm of the aqueous suspension of **1-Eu** (a, b and c) and **1-Tb** (d, e and f) in the presence of Fe^{3+}, CrO_4^{2-} and $Cr_2O_7^{2-}$ at different concentrations.

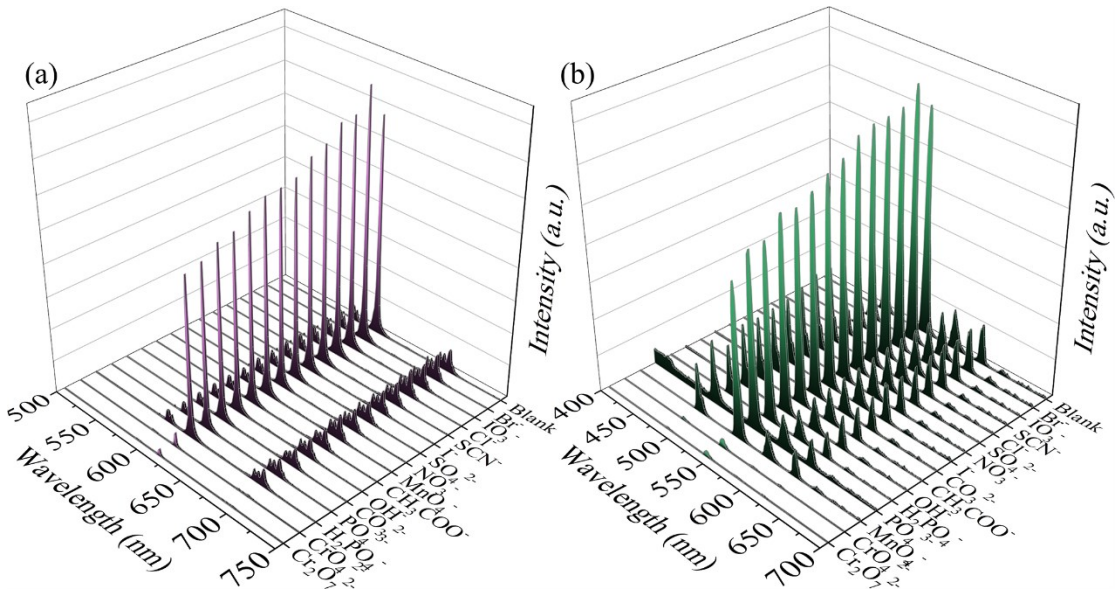

Fig. S13 Emission spectra of **1-Eu** (a) and **1-Tb** (b) immersed in anion aqueous solutions.

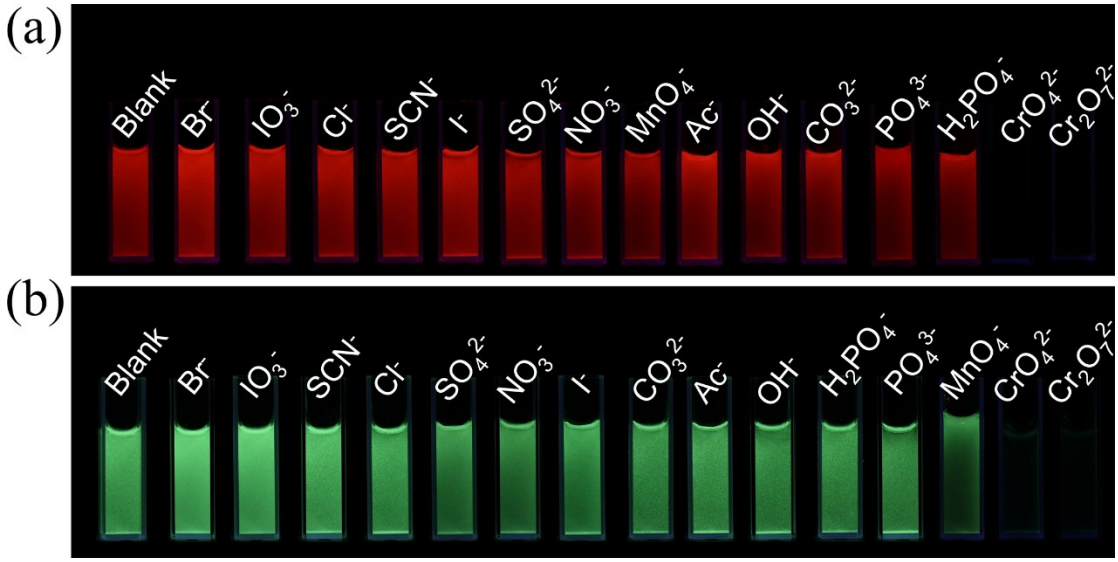

Fig. S14 The photographs of the aqueous dispersed **1-Eu** (a) and **1-Tb** (b) in the presence of different anions under UV irradiation.

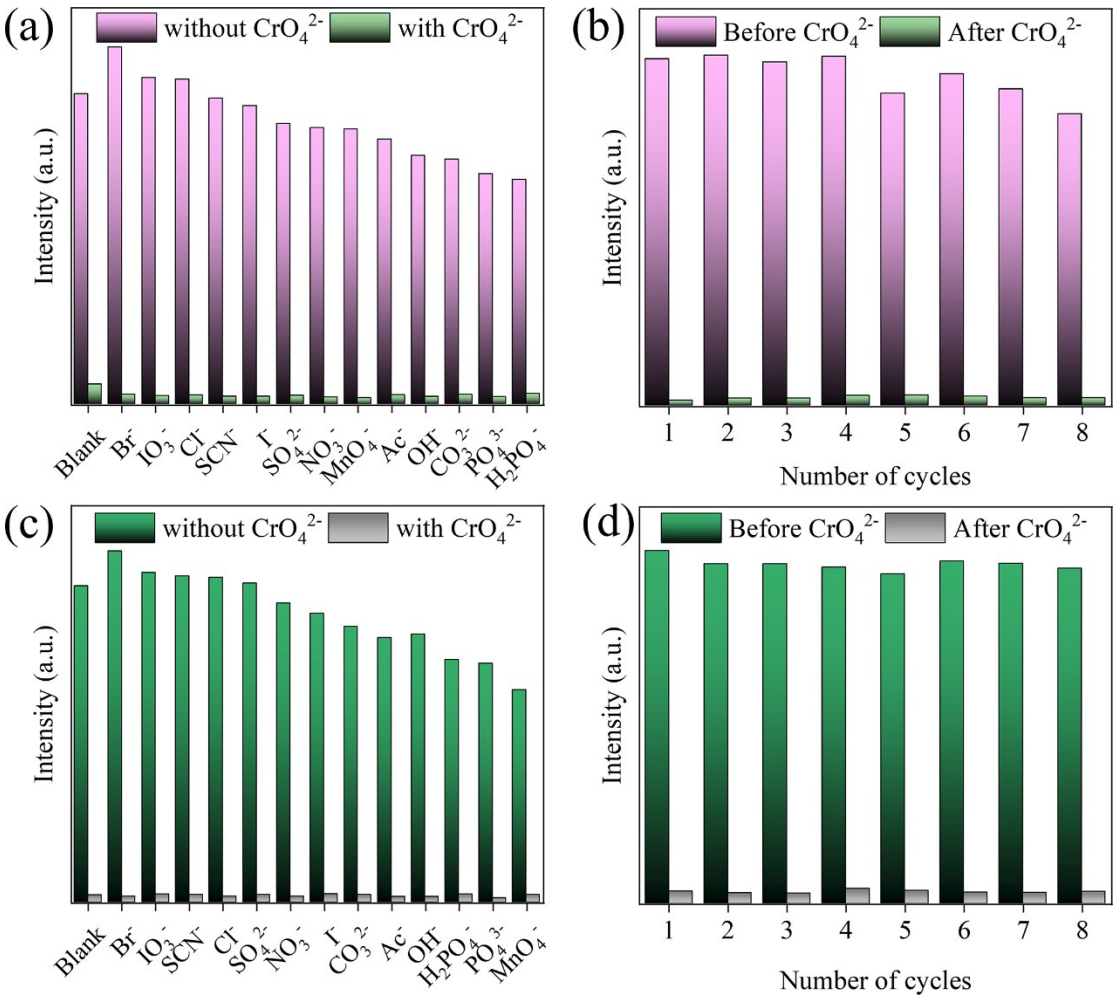

Fig. S15 (a) Luminescent responses of **1-Eu** with mixed-anions (1 mM) in aqueous solutions. (b) Eight cycles test by measuring the luminescent intensity at 617 nm of **1-Eu** before and after the adding of CrO_4^{2-} (1 mM). (c) Luminescent responses of **1-Tb** with mixed-cations (1 mM) in aqueous solutions. (d) Eight cycles test by measuring the luminescent intensity at 545 nm of **1-Tb** before and after the adding of CrO_4^{2-} (1 mM).

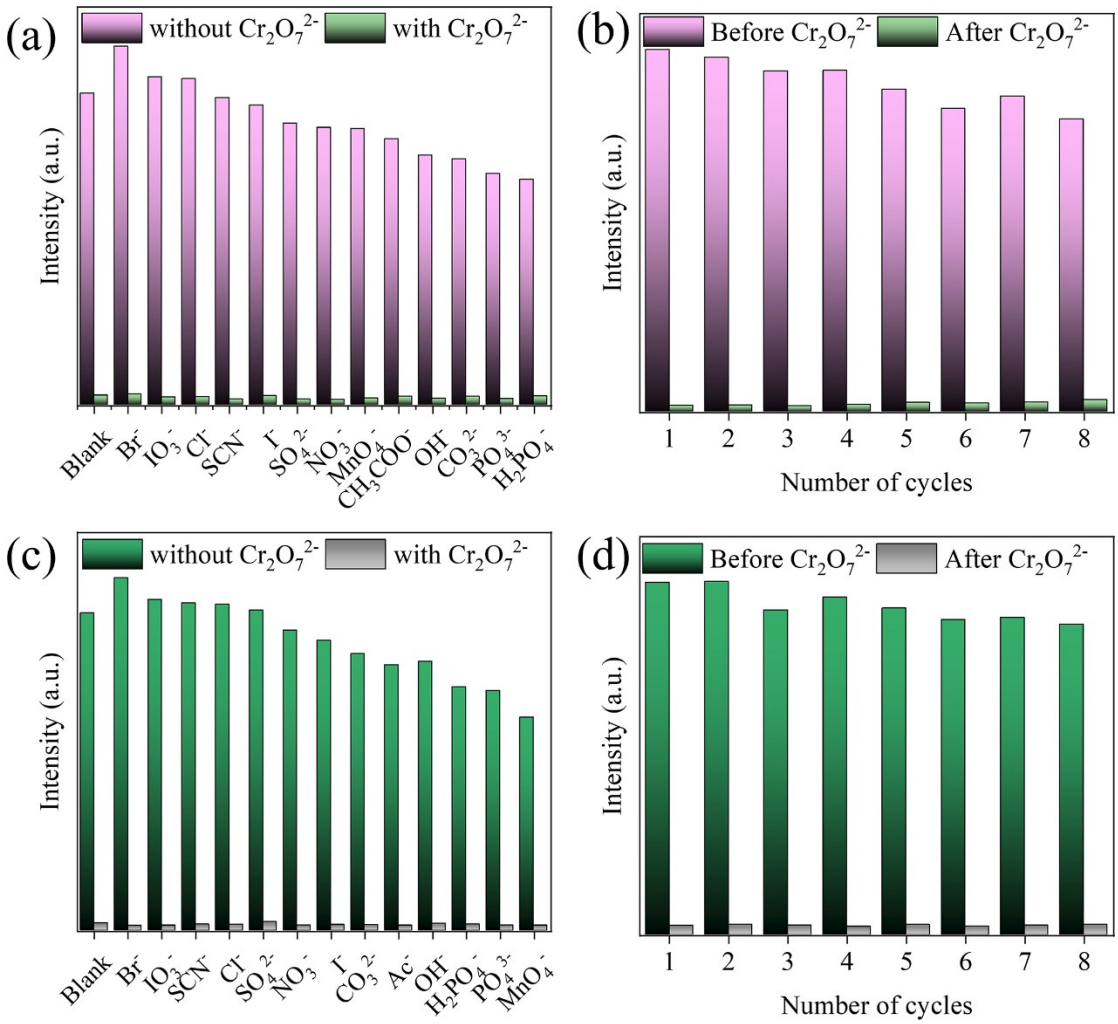

Fig. S16 (a) Luminescent responses of **1-Eu** with mixed-anions (1 mM) in aqueous solutions. (b) Eight cycles test by measuring the luminescent intensity at 617 nm of **1-Eu** before and after the adding of $Cr_2O_7^{2-}$ (1 mM). (c) Luminescent responses of **1-Tb** with mixed-cations (1 mM) in aqueous solutions. (d) Eight cycles test by measuring the luminescent intensity at 545 nm of **1-Tb** before and after the adding of $Cr_2O_7^{2-}$ (1 mM).

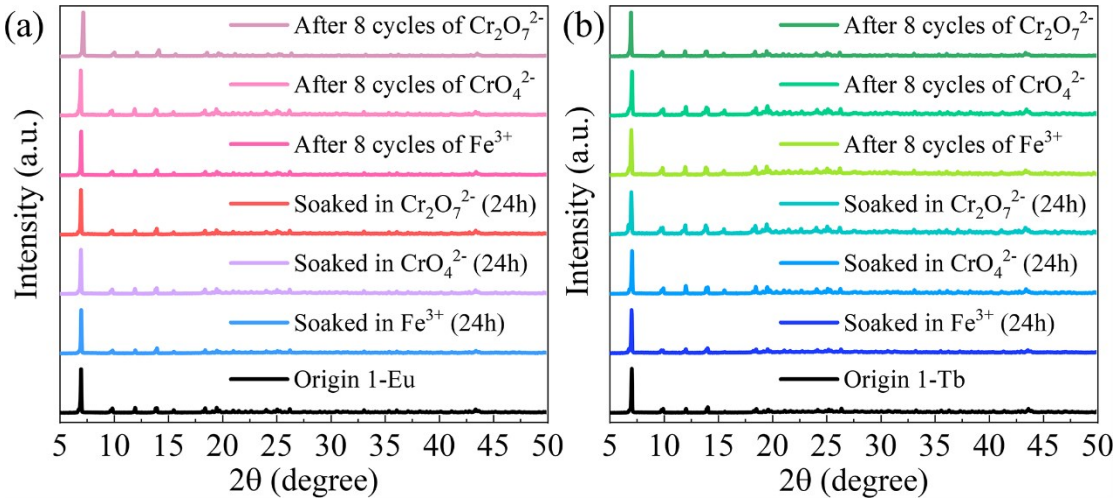

Fig. S17 The PXRD patterns of **1-Eu** (a) and **1-Tb** (b) after using eight cycles and soaked in aqueous Fe^{3+} and $CrO_4^{2-}/Cr_2O_7^{2-}$ solution (1 mM) for 24 h.

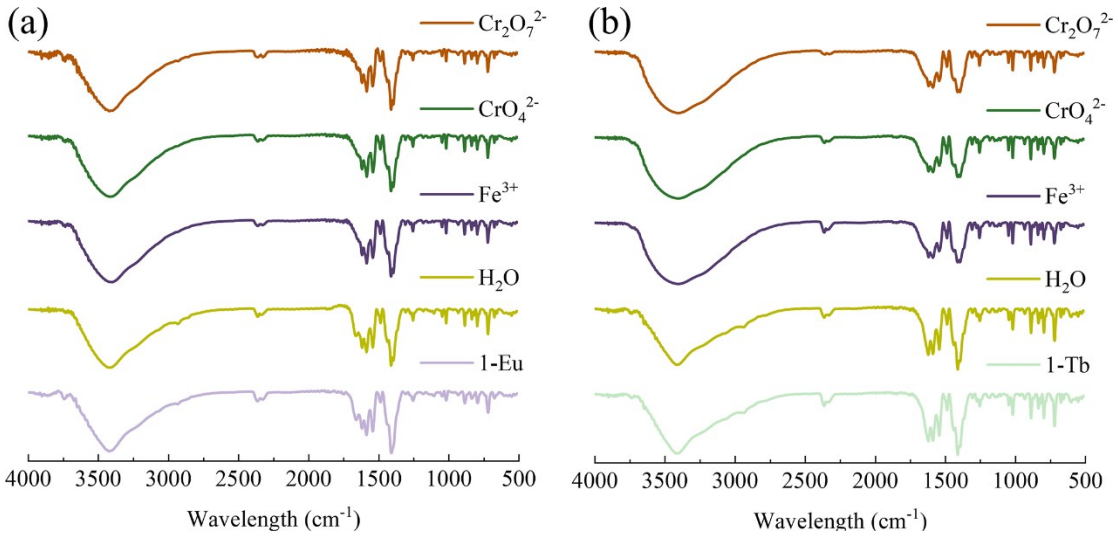

Fig. S18 IR spectra of 1-**Eu** (a), 1-**Tb** (b) in different solution.

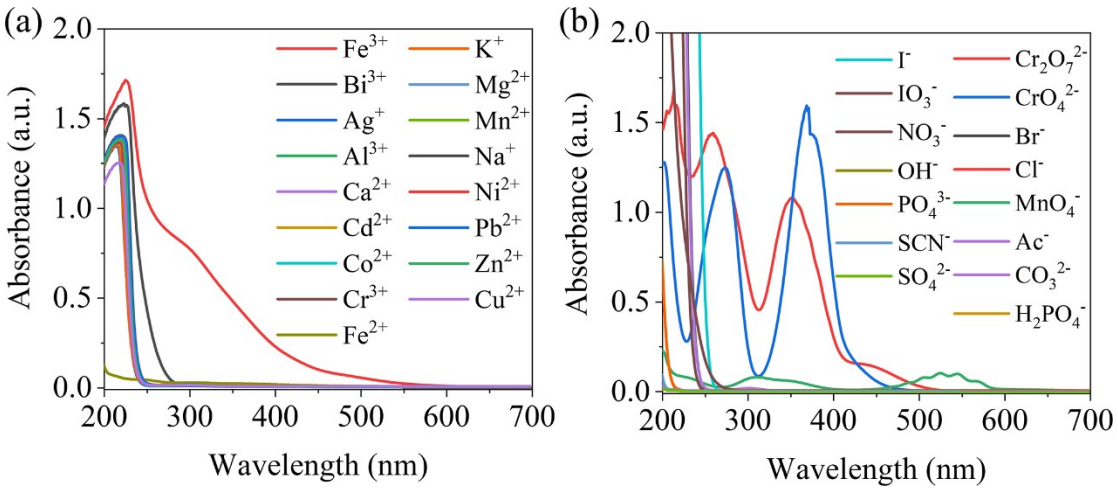

Fig. S19 The UV–Vis absorption spectrum of aqueous solutions of different testing cations (a), anions (b).

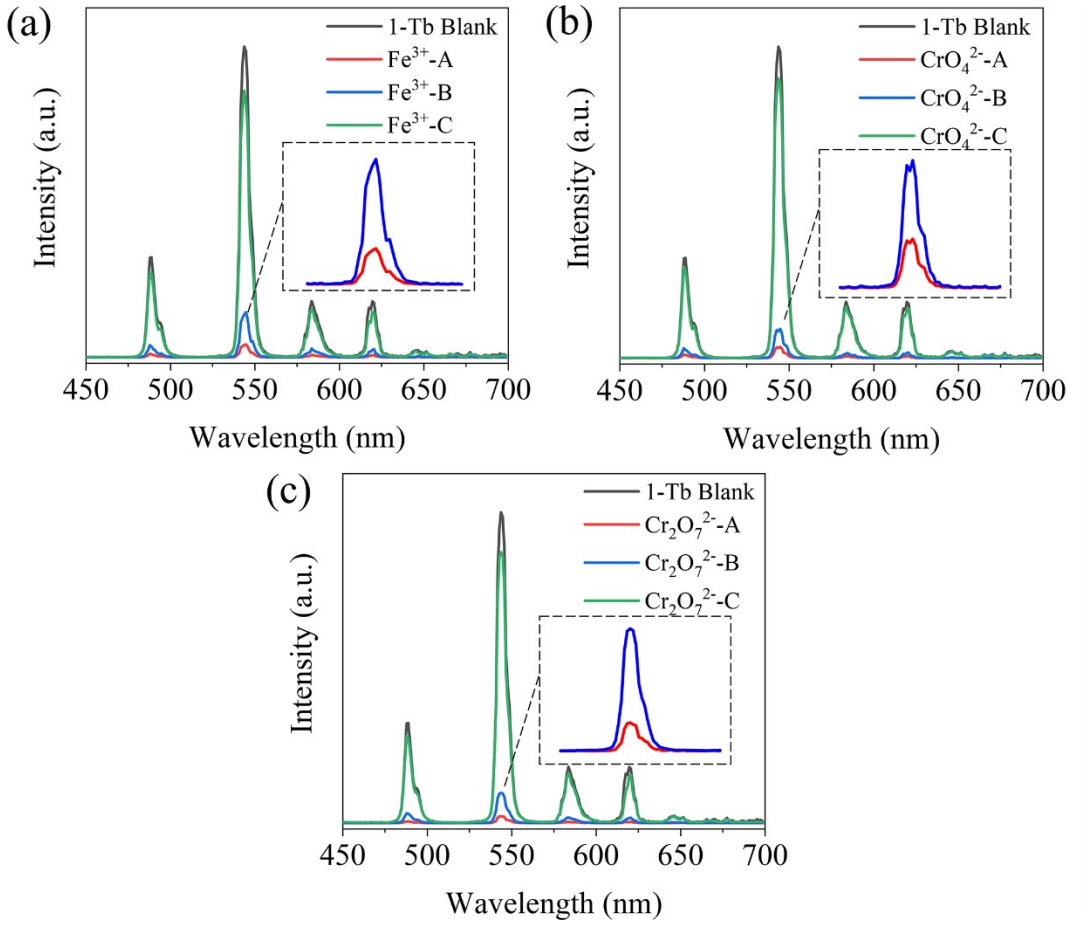

Fig. S20 The emission spectra of **1-Tb** with (a) Fe^{3+}, (b) CrO_4^{2-}, and (c) $Cr_2O_7^{2-}$. (Black curves, **1-Tb** solely in position A; red curves, mixture of **1-Tb** and Fe^{3+} and CrO_4^{2-}/$Cr_2O_7^{2-}$ ions in position A; blue curves, **1-Tb** in position A while Fe^{3+} and CrO_4^{2-}/$Cr_2O_7^{2-}$ ions in position B; green curves, **1-Tb** in position A while Fe^{3+} and CrO_4^{2-}/$Cr_2O_7^{2-}$ ions in position C.)

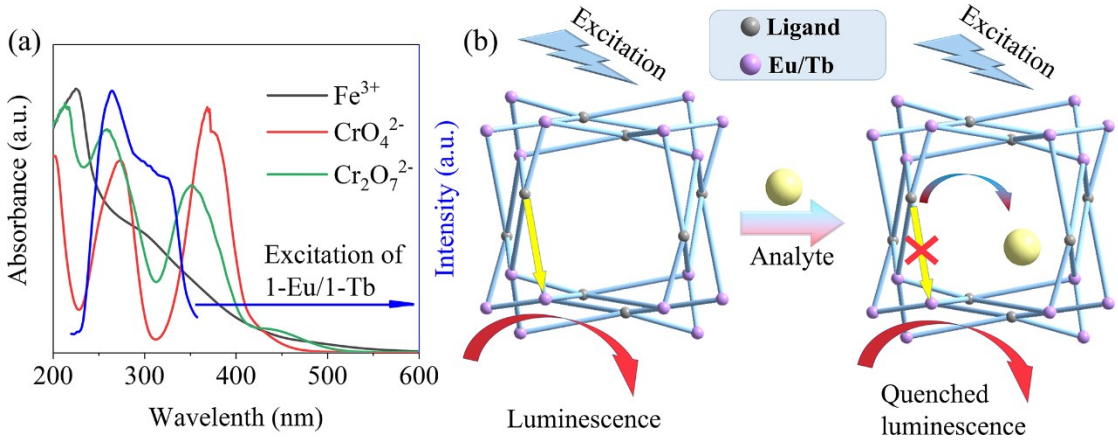

Fig. S21 (a) The overlap between the UV-vis spectra of Fe^{3+}/CrO_4^{2-}/$Cr_2O_7^{2-}$ in aqueous solutions and the excitation spectrum of **1-Eu/1-Tb**. (b) The schematic illustration of the mechanism of **1-Eu/1-Tb** sensing for the analytes.

Table S5. A comparison of quenching constants and corresponding LODs for various luminescent MOFs used for detection of Fe^{3+}.

Materials	solvent	$K_{sv}(M^{-1})$	Detection limit (μM)	Reference
1-Eu	water	2.78×10^4	0.67	This work
1-Tb	water	1.48×10^4	1.26	This work
$[Cd(NDA)(L)(H_2O)_2]_n$	water	4.0×10^4	2.06	*J. Mater. Chem. C,* 2020, **8**, 1427-1432.
$[Ln(L_2)(H_2O)(DMF)]_n$	water	3.10×10^4	1.57	*ACS Appl. Mater. Interfaces,* 2019, **11**, 7914-7926.
DPYBT	water	—	3.04	*Sens. Actuators, B*, 2020, **320**, 128377-128386.
IISERP-MOF25	water	1.52×10^4	12.3	*ACS Appl. Nano Mater*, 2019, **2**, 5169-5178.
Eu-MOF	water	2.028×10^4	—	*Inorg. Chem.,* 2020, **59**, 2005-2010.
Tb-MOF	water	1.204×10^4	—	*Inorg. Chem.,* 2020, **59**, 2005-2010.
534-MOF-Tb(L_{11})	water	5.51×10^3	130	*J. Mater. Chem. C*, 2017, **5**, 2015-2021.
Zn−MOF	water	1.326×10^4	0.882	*Inorg. Chem.,* 2020, **59**, 8818-8826.
[Eu(O-cpia)(phen)]	water	—	300 ppm	*Sens. Actuators, B,* 2018, **258**, 358-364.
BUT-15	water	1.66×10^4	0.3	*ACS Appl. Mater. Interfaces*, 2017, **9**, 10286-10295.
$[Zn_2(TPOM)(NDC_)_2]3.5H_2O$	water	1.9×10^4	2	*J. Mater. Chem. A*, 2016, **4**, 15494-15500.
$[Eu(L)(H_2O)]\cdot 1.5H_2O$	water	6.6×10^4	0.87	*New. J. Chem.*, 2018, **42**, 19485-19493.
FJI-C8 (Zn)	water	8.2×10^3	23.3	*Dalton Trans.,* 2018, **47**, 3452-3458.
$\{[Cd_2(bptc)(phen)_2]\cdot 4H_2O\}n$	water	3.07×10^3	21.7	*Inorg. Chem.,* 2017, **56**, 11768-11778.
$Eu_2(MFDA)_2(HCOO)_2(H_2O)_6$	DMF	1.58×10^3	0.3	*Dalton Trans.* 2013, **42**, 12403-12409.
MOF-808-Tb	water	3.12×10^4	—	*Chem. Commun.,* 2019, **55**, 4727-4730.
$[Zr_6O_4(OH)_4(C_8H_2O_4S_2)_6]\cdot DMF\cdot 18H_2O$	water	4.41×10^3	1.26	*Dalton Trans.,* 2018, **47**, 1159-1170.
$[Cd_2Na(L_{15})(BDC)_{2.5}].9H_20$	DMF	1.67×10^4	162ppb	*J. Mater. Chem. A,* 2017, **5**, 15797-15807.

$\{[Cd(5\text{-}asba)(bimb)]\}_n$	water	1.78×10^4	—	*J. Mater. Chem. C*, 2016, **4**, 11404-11418.

Table S6. A comparison of quenching constants and corresponding LODs for various luminescent MOFs used for detection of $CrO_4^{2-}/Cr_2O_7^{2-}$.

Materials	Analytes	solvent	Detection limit (μM)	Reference
1-Eu	CrO_4^{2-}/ CrO_7^{2-}	water	0.53/0.32	This work
1-Tb	CrO_4^{2-}/ CrO_7^{2-}	water	0.75/0.57	This work
USTC-5	CrO_4^{2-}/ CrO_7^{2-}	water	11.4/1.45	*J. Mater. Chem. C*, 2020, **8**, 11786-11795
$\{[Zn_2L_2(H_2O)_4]\cdot H_2O\}_n$	CrO_4^{2-}/ CrO_7^{2-}	water	2.3 / 2.6	*Dalton Trans.*, 2019, **48**, 387-394.
$[(CH_3)_2NH_2][In(TNB)_{4/3}]\cdot(2DMF)(3H_2O)$	CrO_7^{2-}	water	45	*J. Mater. Chem. C.*, 2018, **6**, 6440–6448.
$[Zn(NH_2\text{-}bdc)(4,4'\text{-}bpy)]$	CrO_4^{2-}/ CrO_7^{2-}	water	2.21/1.3	*Sens. Actuators, B,* 2019, **284**, 403-413.
Zn-MOF	CrO_4^{2-}/ CrO_7^{2-}	water	1.07/1.04	*Inorg. Chem.*, 2020, **59**, 8818-8826.
Zn-MOF-1	CrO_4^{2-}/ CrO_7^{2-}	water	4.8/3.53	*J. Mater. Chem. A,* 2017, **5**, 20035-20043.
$[Zn_2(L_1)(L_2)_2]\cdot 4H_2O$	CrO_4^{2-}/ CrO_7^{2-}	DMF	4.8/3.9	*J. Mater. Chem. A*, 2016, **4**, 15494-15500.
$\{[Zn_3(mtrb)_3(btc)_2]\cdot 3H_2O\}_n$	CrO_4^{2-}/ CrO_7^{2-}	water	4.52/2.83	*Dalton Trans.*, 2018, **47**, 6189–6198.
$[Zn(tpbpc)_2]\cdot$solvent	CrO_4^{2-}/ CrO_7^{2-}	water	0.47 / 0.68	*Sens. Actuators, B,* 2018, **269**, 164-172.
$Zr_6O_4(OH)_7(H_2O)_3(btba)_3$	CrO_7^{2-}	water	1.57	*ACS Appl. Mater. Interfaces,* 2018, **10**, 16650-16659.
$[Zn_3(bpanth)(oba)_3]\cdot 2DMF$	CrO_4^{2-}/ CrO_7^{2-}	water	2.67/1.85	*Chem.-Eur. J.*, 2018, **24**, 3192-3198.
$[Eu_7(mtb)_5(H_2O)_{16}](NO_3)(DMA)_8(H_2O)_{18}$	CrO_4^{2-}	water	3.5 nM	*ACS Appl. Mater. Interfaces,* 2017, **9**, 16448-16457.
$[Cd(TIPA)_2(ClO_4)_2](DMF)_3(H_2O)$	CrO_7^{2-}	water	27nM	*Dalton Trans.*, 2018, **47**, 3725-3732.
Eu^{3+}@MIL-124	CrO_7^{2-}	water	0.15	*ACS Appl. Mater. Interfaces,* 2015, **7**, 721-729.
NU-1000	CrO_7^{2-}	water	1.8	*Inorg. Chem.*, 2017, **56**, 14178-14188.

References

1 Y. J. Cui, H. Xu, Y. F. Yue, Z. Y. Guo, J. C. Yu, Z. X. Chen, J. K. Gao, Y. Yang, G. D. Qian and B. L. Chen, *J. Am. Chem. Soc*., 2012, **134**, 3979–3982.

2 G. M. Sheldrick, Program for Empirical Absorption Correction of Area Detector Data, University of Göttingen, Germany, 1996.

3 G. M. Sheldrick, SHELXS-97, Program for Crystal Structure Solution, Göttingen University, Göttingen, Germany, 1997.

4 S. Alvarez, P. Alemany, D. Casanova, J. Cirera, M. Llunell and D. Avnir, *Coord. Chem. Rev.*, 2005, **249**, 1693–1708.